✕USCAP

ARTICLE

Clinical, histopathologic, and immunoarchitectural features of dermatopathic lymphadenopathy: an update

Sofia Garces[1,2] · C. Cameron Yin[1] · Roberto N. Miranda ⬤[1] · Keyur P. Patel[1] · Shaoying Li ⬤[1] · Jie Xu ⬤[1] · Beenu Thakral[1] · Robert J. Poppiti[2] · Ana Maria Medina[2] · Vathany Sriganeshan[2] · Amilcar Castellano-Sánchez[2] · Joseph D. Khoury ⬤[1] · Juan Carlos Garces[3] · L. Jeffrey Medeiros[1]

Abstract

Dermatopathic lymphadenopathy is a distinctive form of paracortical lymph node hyperplasia that usually occurs in the setting of chronic dermatologic disorders. The aim of this study is to update our understanding of the clinicopathologic and immunophenotypic features of dermatopathic lymphadenopathy. The study cohort was 50 lymph node samples from 42 patients diagnosed with dermatopathic lymphadenopathy. The patients included 29 women and 13 men with a median age of 49 years (range, 12–79). Twenty-two (52%) patients had a dermatologic disorder, including mycosis fungoides ($n = 6$), chronic inflammatory dermatoses ($n = 13$), melanoma ($n = 1$), squamous cell carcinoma ($n = 1$), and Kaposi sarcoma in the context of human immunodeficiency virus infection ($n = 1$). Twenty (48%) patients did not have dermatologic manifestations. Lymph node biopsy specimens were axillary ($n = 22$), inguinal ($n = 21$), cervical ($n = 4$), and intramammary ($n = 3$). All lymph nodes showed paracortical areas expanded by lymphocytes; dendritic cells, including interdigitating dendritic cells and Langerhans cells; and macrophages. Melanophages were detected in 48 (98%) lymph nodes. Immunohistochemical analysis provided results that are somewhat different from those previously reported in the literature. In the paracortical areas of lymph node, S100 protein was expressed in virtually all dendritic cells, and CD1a was expressed in a significantly greater percentage of cells than langerin (80 vs. 35%, $p < 0.0001$). These results suggest that the paracortical regions of dermatopathic lymphadenopathy harbor at least three immunophenotypic subsets of dendritic cells: Langerhans cells (S100$^+$, CD1a$^{+(high)}$, langerin$^+$), interdigitating dendritic cells (S100$^+$, CD1a$^{+(low)}$, langerin$^-$), and a third (S100$^+$, CD1a$^-$, langerin$^-$) minor population of dendritic cells. Furthermore, in more than 60% of dermatopathic lymph nodes, langerin highlighted trabecular and medullary sinuses and cords, showing a linear and reticular staining pattern, which could be a pitfall in the differential diagnosis with Langerhans cell histiocytosis involving lymph nodes.

✉ L. Jeffrey Medeiros
  ljmedeiros@mdanderson.org

[1] Department of Hematopathology, The University of Texas MD Anderson Cancer Center, Houston, TX, USA

[2] Department of Pathology, Mount Sinai Medical Center and The Florida International University Herbert Wertheim College of Medicine, Miami, FL, USA

[3] Instituto Oncológico Nacional Dr. Juan Tanca Marengo, Guayaquil, Ecuador

Introduction

Dermatopathic lymphadenopathy is a distinctive pattern of paracortical lymph node hyperplasia that typically occurs in the setting of chronic skin diseases [1–3]. The original description of dermatopathic lymphadenopathy is attributed mainly to Pautrier and Woringer, who in 1937 named the entity lipomelanotic reticulosis (*réticulose lipo-mélanique*), a term describing the expansion of nodal interfollicular regions by collections of melanin- and fat-containing reticular elements (i.e. histiocytic cells) in a series of patients with lymphadenopathy and erythroderma of various etiologies [3, 4]. In 1942, Hurwitt coined the term dermatopathic lymphadenitis, since it was postulated that the entity represented a secondary immune response to a pathologic condition affecting primarily the skin [1].

In recent years, much has been learned about the immunophysiology underlying the histologic features of dermatopathic lymphadenopathy [5–9]. Evaluation of antigen-presenting dendritic cell subsets present in healthy and chronically inflamed skin, as well as in skin-draining lymph nodes, suggests that cutaneous Langerhans cells and other types of dendritic cells migrate to the T-cell rich areas of regional lymph nodes where they mediate an appropriate immune response [1, 5–8, 10]. This migration occurs in response to persistent antigenic stimuli with subsequent local production of cytokines, such as tumor necrosis factor-alpha, that downregulate epithelial adhesion molecules facilitating migration. Moreover, the characteristic accumulation of melanophages in dermatopathic lymph nodes might result, at least in some cases, from pigmentary incontinence and enhanced melanophagocytosis in inflamed skin, with subsequent migration of melanophages through lymphatic vessels to lymph nodes [8, 10–12].

Except for a few studies published nearly three decades ago, only isolated reports have systematically evaluated the clinicopathologic and immunophenotypic features of dermatopathic lymphadenopathy [1, 8, 10, 13–18]. In this study, we aim to provide an update on the clinicopathologic and immunophenotypic features of dermatopathic lymphadenopathy.

Materials and methods

Study group

The study cohort included 50 lymph node samples from 42 patients diagnosed with dermatopathic lymphadenopathy. Only lymph nodes without overt morphologic evidence of involvement by B- or T-cell lymphoma were included in the study group. In every case, the lymph nodes were clinically abnormal, defined as 1.5 cm or larger in the longest transverse diameter or, regardless of size, being firm, irregular, clustered, or fixed on physical examination [19]. Available paraffin blocks or unstained slides from 20 lymph node samples were retrieved from the archives of the Department of Hematopathology at The University of Texas MD Anderson Cancer Center from January 1, 2009 through December 31, 2017. In addition, paraffin blocks of 30 lymph node samples were culled from the archives of the Department of Pathology at Mount Sinai Medical Center from January 1, 2011 through December 31, 2018. Available clinical and laboratory data were retrieved from the medical records. The study was conducted under Institutional Review Board–approved protocols.

Histologic evaluation

Hematoxylin and eosin (H&E)-stained slides were obtained from formalin-fixed, paraffin-embedded tissue sections, including 42 excisional and 8 core biopsy specimens of lymph nodes with dermatopathic lymphadenopathy. All lymph node specimens were independently reviewed by three authors. Dermatopathic lymphadenopathy was defined morphologically as expansion of lymph node paracortical areas by a mixed cellular infiltrate including lymphocytes and dendritic cells, the latter with elongated, delicately folded, or twisted nuclear contours and abundant pale eosinophilic cytoplasm. For inclusion in this study, we required paracortical dendritic cells to be arranged in confluent collections of ≥20 cells. This criterion facilitated the distinction between mild dermatopathic lymphadenopathy from nonspecific reactive paracortical hyperplasia, in which dendritic cells are usually evenly and singly scattered imparting a starry-sky appearance. Dermatopathic lymph nodes also harbor other immune cells including macrophages, plasma cells, and eosinophils. The presence of melanin pigment was not considered as an inclusion or exclusion criterion; nor was the coexistence or lack of a dermatologic disorder [1, 2, 4, 13, 14].

The extent of paracortical expansion in H&E-stained sections of lymph nodes with dermatopathic lymphadenopathy was assessed using an Olympus glass eyepiece (WH10×/22) at 200× magnification, and stratified into three categories as follows: mild (category 1), with easily discernible, confluent aggregates of ≥20 dendritic cells that do not exceed a 200× power microscopic field; moderate (category 2), showing confluent aggregates of dendritic cells forming vague nodules or networks broader than a 200× power microscopic field but without compression or peripheralization of cortical lymphoid follicles toward the capsule and/or trabeculae; and severe or "florid" (category 3) dermatopathic lymphadenopathy, with confluent aggregates of dendritic cells forming vague nodules or networks broader than a 200× power microscopic field, and associated with compression and peripheralization of lymphoid cortical follicles toward the capsule and/or trabeculae. The amount of intracytoplasmic melanin, defined as fine, non-refractile dark-brown granules in macrophages, was assessed microscopically at 20× and 600× magnification and was not considered in the grading system. When present, the amount of melanin pigment was semi-quantified as follows: abundant, when the pigment was obvious at low power (20×) magnification; scant, when the pigment was only recognized after careful examination at high (600×) magnification; and moderate, when the amount was between these two extremes. We also assessed microscopically, at 600× magnification, for the presence of other types of intracytoplasmic

pigmented particles in macrophages, including hemosiderin, recognized as refractile golden-yellow to golden-brown globular particles; and tattoo pigment, identified as coarse black non-refractile granules.

The presence of atypical lymphocytes with cerebriform or hyperconvoluted nuclei was assessed in every case using an Olympus glass eyepiece (WH10X/22) at 1000× magnification under oil immersion and categorized using the National Cancer Institute-Veterans Administration Hospital classification (NCI-VA); as follows: LN0, no atypical (cerebriform) lymphocytes; LN1, occasional and isolated atypical lymphocytes; LN2, many atypical lymphocytes in clusters of three to six cells and LN3, aggregates of atypical lymphocytes with preserved nodal architecture [19]. Cases were also classified according to the International Society for Cutaneous Lymphomas/European Organization for Research and Treatment of Cancer (ISCL/EORTC) staging system [19]. By definition, no cases with partial or complete effacement of the nodal architecture by atypical lymphocytes or frankly neoplastic cells that would have been classified as stage LN4 (NCI) or stage N3 (ISCL/EORTC) were included in this study. Paracortical eosinophils, neutrophils, plasma cells, and mitotic figures were quantified as the average number in ten high power fields (400×) and classified as 0 (absent), 1+ (1–3 per high power field), 2+ (4–5 per high power field), and 3+ (>5 per high power field). We also assessed for the presence of reactive follicular hyperplasia defined as one or more hyperplastic follicles with germinal centers; and, for the presence of Castleman-like changes, defined as the presence of three or more follicles with both regressive changes and onion skin-like mantle zones. We additionally evaluated the vascular architecture of dermatopathic lymph nodes; and assessed for the presence of capsular and/or trabecular fibrosis.

Immunohistochemistry and flow cytometry

Immunohistochemical studies were performed on fixed, paraffin-embedded tissue sections using different systems in each of the two institutions. At MD Anderson Cancer Center, we used an automated immunostainer (BOND III: Leica Biosystems, Buffalo Grove, IL, USA) as described previously [20]. At Mount Sinai Medical Center, immunohistochemical analysis was carried out in a Ventana automated immunostainer (Ventana BenchMark Ultra, Tucson, AZ, USA) as described previously [21]. The following antibodies, some of which differed in the two institutions, were used on all 50 lymph node specimens: CD1a (Leica Biosystem, Newcastle, UK; or Cell Marque, Rocklin, CA, USA); S100 protein (BioGenex, Fremont, CA, USA; or Cell Marque), and langerin (CD207) (clone 12D6, Novocastra/Vision Biosystem, Benton Lane, Newcastle-upon-Tyne, UK). Additional antibodies were used on smaller

subsets of lymph node specimens including: CD21 (Leica Biosystem; or Cell Marque); CD30, CD163, E-Cadherin (DAKO, Carpinteria, CA, USA; or Cell Marque); CD68 (clone KP1, DAKO, Glostrup, Denmark; or Cell Marque); BRAF V600E (VE-1) (Spring Bioscience, Pleasanton, CA, USA); cyclin D1 (clone SP4, Labvision/Neomarkers, Fremont, CA, USA; or clone SP4-R, Ventana, Tucson, AZ, USA); anti-Ki-67 (Ventana); and the highly specific p-ERK antibody (anti-phospho-p44/42 MAPK [Erk1/2] [Thr202/Tyr204]) (clone D13.14.4E, dilution 1:300, Cell Signaling, Danvers, MA, USA); CD11c and CD33 (Novocastra/Vision Biosystem); CD123 (Leica Biosystem); and desmin, smooth muscle, actin and vimentin (Ventana).

Using antibodies specific for CD1a, CD11c, CD21, CD33, CD68, CD163, E-cadherin, langerin, and S100-protein, we quantified the approximate percentage of positive cells among the total number of histiocytic cells (including dendritic cells and macrophages) colonizing each of three main lymph node compartments (i.e. cortex, paracortex, and sinuses) by visualization at 100× and 400× magnification. The approximate percentage of positive cells was rounded to the nearest fifth percentile and recorded. Lymph node samples were considered positive if staining was present in ≥5% of histiocytic cells.

Immunoblasts were defined as CD30-positive medium-sized lymphoid cells with visible nucleoli, quantified in the paracortex as the average in ten high power microscopic fields (X400) and reported as: 0 (absent), (1+) 1 to 4; (2+), 5–15; and (3+) >15 immunoblasts per high power field. In ten lymph node samples with >15 immunoblasts per high power field, we also performed ALK1 and CD15 (Labvision/Neomarkers; or Ventana). The Ki-67 proliferative index was defined as the percentage of positive cells among the total number of cells in the paracortex of dermatopathic lymph nodes, and categorized as: <15%, 15–30%, and >30%.

Flow cytometry immunophenotypic analysis was performed on 24 lymph node samples, including six lymph node samples from six patients with mycosis fungoides. At least four-color analysis was performed on all samples, and lymphocytes were gated using CD45 and side scatter. At MD Anderson Cancer center, standard multicolor analysis was performed using the FACS Canto II instrument (Becton Dickinson, San Jose, CA, USA), and at Mount Sinai Medical Center, using a Beckman Coulter FC500 analyzer (Miami, FL, USA) as described previously [22]. A variable panel of antibodies was used at the two institutions, which included varying combinations of reagents specific for: CD2, CD3, CD4, CD5, CD7, CD8, CD10, CD16, CD19, CD20, CD22, CD23, CD25, CD26, CD30, CD43, CD45, CD52, CD56, CD57, CD94, CD79b, TCR αβ chain, and TCR γδ chain and surface immunoglobulin light chains (Becton–Dickinson; or Beckman Coulter).

Molecular studies

In ten lymph node samples, including all six samples from patients with mycosis fungoides, TRG and TRB were assessed for rearrangements using polymerase chain reaction-based methods on DNA extracted from paraffin-embedded tissues as described previously [23]. In five lymph node samples that were not involved by T-cell lymphoma as demonstrated by both negative flow cytometry immunophenotyping and clonality studies, we performed amplicon-based next-generation sequencing targeting the coding regions of a panel of 146 genes that are commonly mutated in hematopoietic neoplasms using the Ion Torrent platform (Thermo Fisher Scientific, Waltham, MA, USA) using DNA extracted from paraffin-embedded tissues as described previously [24]. A complete list of the genes tested is available in Supplementary file 1. For four sequenced cases, we were able to retrieve tissues that were not involved by dermatopathic lymphadenopathy or lymphoma to be used as a control. We used 20 ng of DNA to prepare the genomic library. Following successful library generation and purification, DNA was used for multiplex sequencing and analyzed using the Torrent Suite and OncoSeek data pipeline.

Statistical analysis

Statistical analysis was performed using GraphPad Prism 8.2.11 (GraphPad Software, La Jolla, CA, USA). Fisher exact test and the Mann–Whitney U test were used to assess categorical and continuous variables, respectively. A $p < 0.05$ was considered statistically significant.

Results

Clinical features

The study group included 29 women and 13 men with a median age of 49 years (range, 12–79). The clinical features and the flow cytometry immunophenotyping and molecular results are summarized in Table 1. All patients had lymphadenopathy; 22 (52%) patients had a dermatologic disorder, including mycosis fungoides ($n = 6$), atopic dermatitis ($n = 6$), psoriasis ($n = 2$), erythrodermic drug reaction related to therapy for classic Hodgkin lymphoma ($n = 2$), stasis dermatitis ($n = 2$), chronic contact dermatitis ($n = 1$), melanoma ($n = 1$), squamous cell carcinoma ($n = 1$), and Kaposi sarcoma in a patient with human immunodeficiency virus infection ($n = 1$). Twenty (48%) patients did not have dermatologic manifestations, including eight patients with breast carcinoma, seven in whom lymphadenopathy was the only clinical finding and one patient each with prostatic

adenocarcinoma, classic Hodgkin lymphoma, monoclonal B-cell lymphocytosis, lipoma of the posterior neck, and non-cutaneous extranodal Rosai–Dorfman disease. In 40 (95%) patients, lymphadenopathy was discovered during physical examination or by imaging studies performed for the assessment of dermatologic or non-dermatologic disease including mammography, magnetic resonance imaging, computed tomography, and/or positron emission tomography scans. In one patient (#17), the enlarged lymph node was an incidental finding detected by computed tomography scan performed following a motor vehicle accident. One patient (#36) had an enlarged lymph node detected during routine screening mammogram.

Lymphadenopathy was exclusively axillary in 15 (36%), inguinal in six (14%) and cervical in three (7%) patients. Ten (24%) patients had lymphadenopathy involving the axillary and inguinal regions; three (7%) patients had axillary and ipsilateral intramammary lymphadenopathy, and five (12%) patients had multicompartmental lymphadenopathy, including axillary, inguinal, and cervical regions. Among the latter group, two patients also had mediastinal lymphadenopathy. Lymphadenopathy was bilateral in 23 (55%) patients and unilateral in 19 (45%) patients. Lymph node biopsy specimens were axillary in 22 (44%), inguinal in 21 (42%), cervical in 4 (8%), and intramammary in 3 (6%) cases. In patients with a history of dermatologic disorders, the median interval from onset of dermatologic manifestations to detection of dermatopathic lymphadenopathy was 28 months (range, 1–207 months). Lymph nodes were not tender on palpation in 38 (90%) patients; 4 (10%) patients had tender lymph nodes (patients # 9, #36, #37, and #42). Radiologically, the maximal diameter of the largest lymph node in each patient ranged from 1 to 3.5 cm (median, 1.8 cm). None of the patients had bone or lung lesions on radiologic examination.

Clinical follow-up data were available for 29 patients. The median follow-up time was 33 months (range, 1–92 months). Among eight patients who underwent subsequent lymph node biopsy, 5 (#4, #7, #28, #30 and #41) showed persistent dermatopathic lymphadenopathy. None of the patients with associated benign dermatologic diseases and available follow-up data developed cutaneous lymphoma. Thirteen patients were lost to follow-up.

Histologic features

All lymph nodes showed expanded paracortical regions by a mixed cellular infiltrate that included lymphocytes, variably sized aggregates of dendritic cells and occasional macrophages. Langerhans cells were morphologically indistinguishable from other dendritic cell subsets; these cells had ill-defined cell borders, elongated and delicately folded or twisted nuclear contours with occasional nuclear grooves,

Table 1 Clinical features, flow cytometry immunophenotyping and molecular results in patients with dermatopathic lymphadenopathy.

Patient no.	Age[a]	Sex	Associated disease	Interval from skin disease to DL (months)	LAD anatomic distribution	FC of LN with DL	PCR analysis of TRG and TRB genes	NGS results
1	23	F	MF	55	Bilateral, multicompartmental	Negative	Polyclonal	No mutations
2	43	M	MF	6	Unilateral axillary	Negative	Polyclonal	No mutations
3	64	F	AD	78	Bilateral axillary and inguinal	Negative	Polyclonal	No mutations
4	48	F	AD	13	Bilateral, multicompartmental	Negative	Polyclonal	No mutations
5	50	M	Chronic contact dermatitis	81	Bilateral axillary and inguinal	Negative	Polyclonal	NA
6	55	F	Breast carcinoma	NA	Unilateral axillary	NA	NA	NA
7	12	M	Erythrodermic drug eruption[b]	20	Unilateral axillary and inguinal	Negative	NA	No mutations
8	59	F	Breast carcinoma	NA	Unilateral axillary	NA	NA	NA
9	19	M	AD	68	Bilateral axillary and inguinal	Negative	NA	NA
10	28	F	Non-cutaneous RDD	NA	Bilateral inguinal	Negative	NA	NA
11	44	F	Melanoma	6	Bilateral axillary and inguinal	NA	NA	NA
12	46	M	No significant[c]	NA	Unilateral axillary	NA	NA	NA
13	36	M	Erythrodermic drug eruption[b]	62	Bilateral axillary	NA	NA	NA
14	69	M	CLL-type MBL	NA	Bilateral axillary	Negative	NA	NA
15	71	F	MF	207	Bilateral axillary	Negative	Polyclonal	NA
16	30	F	CHL	NA	Unilateral axillary	NA	NA	NA
17	55	F	No significant[d]	NA	Unilateral axillary	Negative	NA	NA
18	52	F	AD	7	Unilateral inguinal	Negative	NA	NA
19	51	M	MF	13	Bilateral axillary and Inguinal	Negative	Polyclonal	NA
20	54	F	SCC of head and neck	1	Unilateral cervical	NA	NA	NA
21	50	M	HIV-associated Kaposi sarcoma of skin of lower extremities	2	Bilateral, multicompartmental (including mediastinal)	Negative	NA	NA
22	46	F	Breast carcinoma	NA	Unilateral axillary and intramammary	NA	NA	NA
23	40	F	Breast carcinoma	NA	Unilateral axillary	NA	NA	NA
24	79	M	Prostatic adenocarcinoma	NA	Bilateral inguinal	NA	NA	NA
25	72	F	MF	35	Bilateral axillary and inguinal	Positive	Monoclonal	NA
26	38	F	AD	13	Bilateral, multicompartmental	Negative	Polyclonal	NA
27	75	M	Stasis dermatitis of lower extremities[c]	58	Bilateral inguinal	NA	NA	NA
28	48	F	Breast carcinoma	NA	Unilateral axillary	NA	NA	NA
29	48	F	Psoriasis	154	Unilateral cervical	Negative	NA	NA
30	69	F	Breast carcinoma	NA	Unilateral axillary and intramammary	NA	NA	NA
31	23	F	No significant[c]	NA	Bilateral axillary	NA	NA	NA
32	36	F	No significant[c]	NA	Unilateral axillary	NA	NA	NA
33	53	M	Lipoma of posterior neck	NA	Unilateral cervical	NA	NA	NA
34	59	F	Breast carcinoma	NA	Unilateral axillary and intramammary	NA	NA	NA
35	63	F	AD	17	Bilateral, multicompartmental (including mediastinal)	Negative	NA	NA
36	52	F	No significant[d]	NA	Bilateral axillary	Negative	NA	NA
37	48	F	No significant[c]	NA	Unilateral inguinal	Negative	NA	NA
38	51	F	Stasis dermatitis of lower extremities[c]	83	Bilateral inguinal	Negative	NA	NA
39	76	F	MF	16	Bilateral axillary and inguinal	Positive	Monoclonal	NA
40	42	F	No significant[c]	NA	Bilateral axillary and inguinal	Negative	NA	NA
41	27	F	Breast carcinoma	NA	Unilateral axillary	NA	NA	NA
42	43	M	Psoriasis	122	Bilateral axillary and inguinal	Negative	NA	NA

AD atopic dermatitis, *CHL* classic Hodgkin lymphoma, *CLL* chronic lymphocytic leukemia, *DL* dermatopathic lymphadenopathy, *F* female, *FC* flow cytometry immunophenotyping, *HIV* human immunodeficiency virus, *LAD* lymphadenopathy, *LN* lymph node, *M* male, *MBL* monoclonal B-cell lymphocytosis, *m* months, *MF* mycosis fungoides, *NA* not available, *NGS* next-generation sequencing, *PCR* polymerase chain reaction, *RDD* Rosai-Dorfman disease, *SCC* squamous cell carcinoma, *TRB* T-cell receptor beta, *TRG* T-cell receptor gamma

[a]Indicates age at time of diagnosis of dermatopathic lymphadenopathy

[b]The erythrodermic drug eruption was related to therapy for classic Hodgkin lymphoma

[c]Palpable lymphadenopathy in a patient with no other significant medical history

[d]Lymphadenopathy detected incidentally on radiologic imaging

lacy or vesicular chromatin, inconspicuous nucleoli and pale eosinophilic cytoplasm, often with fine vacuoles. (Figs. 1–5) The extent of the nodal paracortical expansion was stratified as follows: mild (category 1) in 13 (26%), moderate (category 2) in 16 (32%) and severe or florid (category 3) in 21 (42%). (Figs. 1–5) Melanophages were present in sinuses and paracortical areas in 48 (98%) lymph node samples, including 11 (22%) with scant, 18 (36%) moderate and 19 (38%) with abundant melanin pigment. In addition, 8 (16%) lymph nodes showed hemosiderin-laden macrophages,
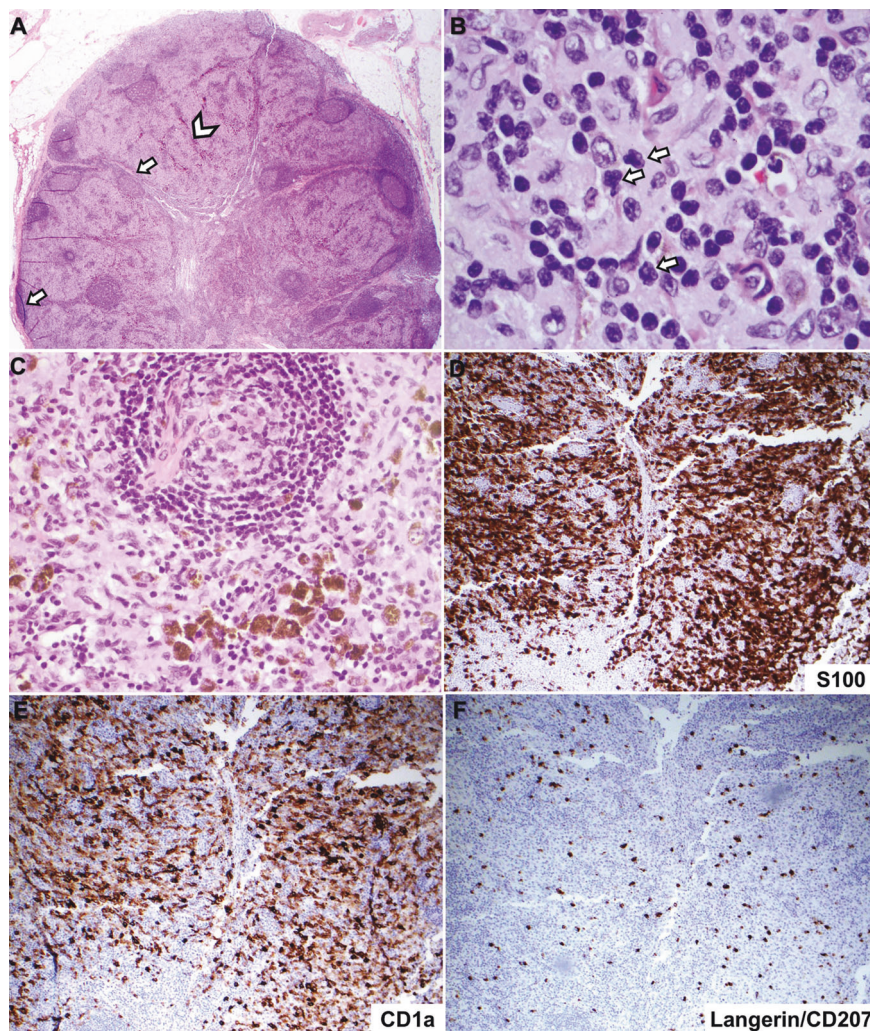
Fig. 1 Florid dermatopathic lymphadenopathy (category 3) associated with mycosis fungoides (Patient #2). a The paracortex is expanded by vaguely nodular, pale-staining cellular aggregates. Follicles are frequently compressed toward the lymph node capsule and trabeculae (arrows). Pigment is observed even at low-power magnification (arrowhead) (20×). **b** Under oil immersion, occasional scattered atypical (cerebriform) lymphocytes are seen in association with a mixed histiocytic infiltrate (arrows), however, flow cytometry immunophenotyping and polymerase chain reaction studies of this lymph node were negative for antigenic aberrancies and T-cell clonality, respectively (1000×). **c** This case showed occasional follicles with Castleman-like changes consisting of regressive changes and onionskin-like mantle zones (400×). **d** The paracortical histiocytic cell infiltrate showed a homogeneous strong and diffuse expression of S100 protein, and **e** CD1a showed heterogeneity in the intensity of staining of paracortical dendritic cells, which comprised about 80% of histiocytic cells (100×). **f** In contrast, langerin/207 highlighted only 10% of the histiocytic infiltrate (100×).

which were discernible only at high power (600×) magnification, and mostly distributed within sinuses and near vessels in the paracortex. None of the lymph nodes analyzed showed tattoo pigment deposits. Lymph nodes from patients with dermatologic disorders more commonly showed severe or florid (category 3) dermatopathic changes vs. patients without associated skin disorders (66% vs. 10%, $p \leq 0.0001$). However, no significant difference in the quantity of melanophages was observed between lymph node samples in the two patient groups.

Paracortical eosinophils were present in 24 (48%) lymph node samples, including 18 (36%) with 1+ and 6 (12%) with 2+ eosinophils. None of the cases showed an average count of more than 5 eosinophils per high power microscopic field (3+) or eosinophilic clustering ("eosinophilic microabscesses"). (Fig. 5a, inset) In 45 (90%) lymph nodes, plasma cells were a part of the paracortical cellular infiltrate, but always infrequent (1+) and scattered (Fig. 3b). In 2 (4%) lymph node samples (cases #7 and #21), neutrophils were part of the mixed paracortical infiltrate, albeit at a low level (1+). In the paracortex, 30 (60%) lymph nodes showed a 1+ mitotic score and 9 (18%) a 2+ mitotic score (Fig. 2c); no lymph nodes showed a mean mitotic count >5 per high power microscopic field (3+). In 38 (76%) lymph nodes, the

Fig. 2 Dermatopathic
lymphadenopathy, moderate
(category 2), associated with
atopic dermatitis (Patient #3).
a The paracortex is expanded by
pale-staining cellular meshworks
without compression of
lymphoid follicles (40×). b The
paracortical infiltrate is
composed of Langerhans cells
and other cytomorphologically
indistinguishable dendritic cells,
macrophages and lymphocytes
including immunoblasts. There
are many thin-walled capillaries.
c Under oil immersion, there are
rare mitotic figures (arrowhead)
(1000×). d This case showed
markedly increased CD30-
positive immunoblasts, without
immunophenotypic aberrancies
(200×). Immunostains for CD15
and ALK1 were negative (not
shown). e The paracortical
dendritic cell infiltrate showed
heterogeneous expression of
CD1a, comprising ~80% of the
total histiocytic cells. f In
contrast, langerin/207
highlighted only 10% of the
histiocytic cell infiltrate (100×).
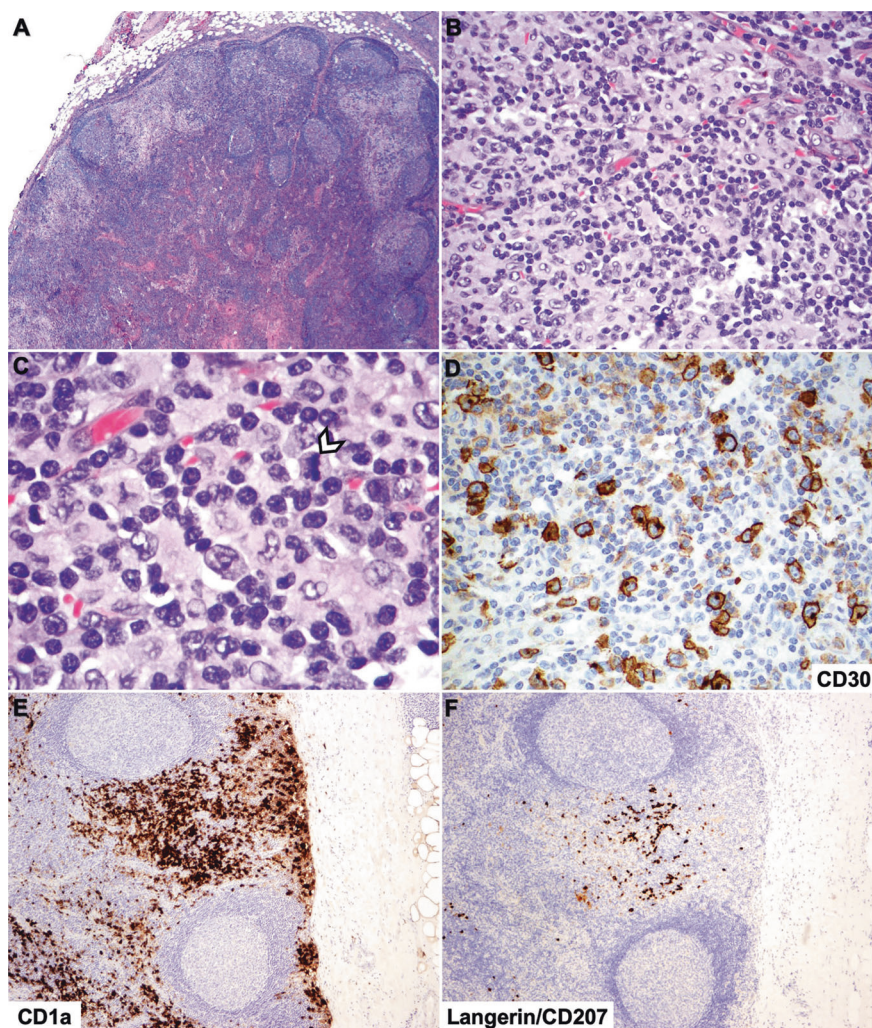
paracortical infiltrate was rich in small, thin-walled, occasionally branching blood vessels. (Figs. 2b, 3b).

In 47 (94%) lymph nodes, the subcapsular, trabecular, and medullary sinuses were patent; however, three (6%) lymph nodes with "florid" (category 3) disease showed partial compression of sinuses by the paracortical infiltrate (Figs. 1a and 5a). When patent, lymph node sinuses harbored numerous histiocytes with and without intracytoplasmic melanin pigment. There was mild to moderate plasmacytosis of the medullary cords in 42 (84%) lymph nodes. Twenty-nine (58%) lymph nodes showed reactive follicular hyperplasia (Figs. 1a, 2a, and 3a) and 18 (36%) lymph nodes showed follicles with Castleman-like changes (Figs. 1c and 3a, inset). There was mild fibrosis of the lymph node capsule and/or fibrous trabeculae in 15 (36%) of 42 excisional lymph node specimens. In two (4%) samples (patients #2 and #10), inguinal lymph nodes also showed a proliferation of thick-walled blood vessels, smooth muscle bundles and fibroblasts in the hilum, diagnostic of angiomyomatous hamartoma. None of the lymph

nodes showed giant cells, granulomas, areas of necrosis, or overt morphologic evidence of involvement by lymphoma. A summary of the histopathologic features of 50 lymph nodes with dermatopathic lymphadenopathy is provided in Table 2.

Immunophenotypic features

All 50 lymph node specimens showed paracortical expansion by mixed populations of dendritic cells that were variably positive for S100 protein, CD1a and langerin. S100 protein was positive in 80–90% (median, 90%) and CD1a in 70–90% (median, 80%) of the total dendritic cells in the paracortex. Of note, whereas S100 protein was homogeneously strong in every lymph node sample (Fig. 1d), the intensity of CD1a expression among individual paracortical dendritic cells was heterogeneous, including subsets of dendritic cells with strong intensity and others with weak to moderate intensity. (Figs. 1e, 2e, 5c and 5c, inset) Conversely, langerin highlighted dendritic cells corresponding
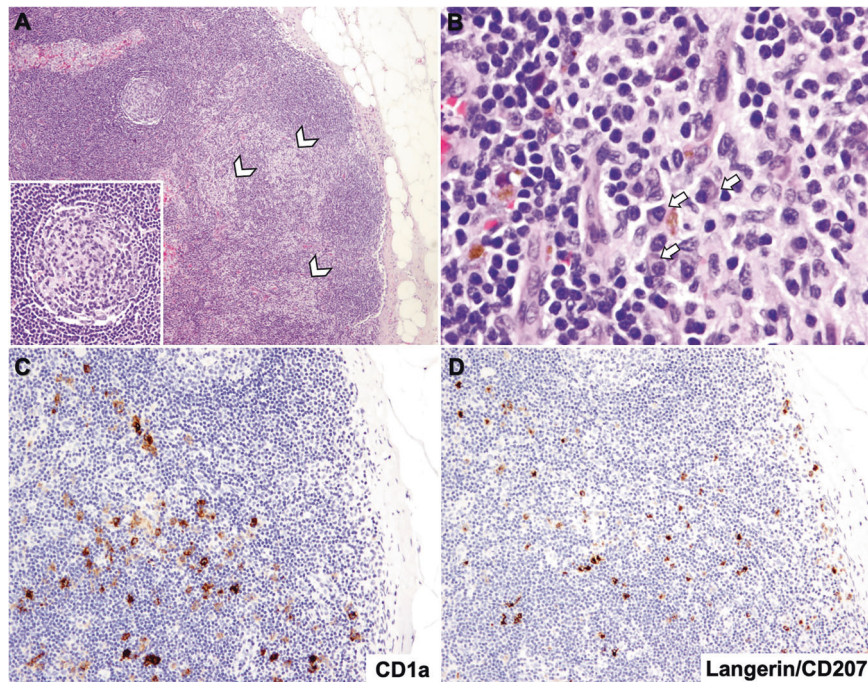
Fig. 3 Dermatopathic lymphadenopathy, mild (category 1), not associated with a dermatologic disorder (Case 17). a There is paracortical colonization by easily discernable, confluent aggregates of at least 20 pale-staining cells in the paracortex (arrowheads). The aggregate did not exceed a 200× power field. This case showed occasional follicles with Castleman-like changes (100×; 400×, inset). **b** The paracortical infiltrate is composed of Langerhans cells, other cytomorphologically indistinguishable dendritic cells, and pigment-laden macrophages. There are many thin-walled capillaries and scattered plasma cells (arrows) **c, d** More than 90% of the paracortical mixed histiocytic cell infiltrate expressed S100 protein (not shown); CD1a was expressed in ~80% of histiocytic cells. In contrast, langerin highlighted only 20% of the histiocytic infiltrate (100×).

to 10–70% (median, 40%) of all paracortical histiocytic cells, a significantly lower proportion of positive cells than those highlighted by CD1a ($p < 0.0001$). (Figs. 1f, 2f, 3d and 5e, inset).

In 40 lymph node samples, a larger battery of antibodies was used. In all samples tested, CD68 and CD163 were positive in macrophages predominately surrounding the trabecular and medullary sinuses, away from the lymph node capsule, and corresponded to 10–25% (median, 15%) of all paracortical histiocytic cells. All lymph node samples tested showed weak expression of E-cadherin by scattered or loose aggregates of paracortical dendritic cells, comprising 5–20% (median, 10%) of paracortical histiocytic cells. CD21 was negative in the paracortex of all lymph nodes tested. Cyclin D1 and p-ERK were negative in paracortical dendritic cells; nevertheless, these markers were expressed in the nuclei of rare macrophages, corresponding to <10% of histiocytic cells in the paracortex. BRAF V600E (VE-1) was negative in the paracortex, cortex and sinuses of all lymph node samples assessed. CD30-positive immunoblasts were scattered in the paracortical regions, with an average count per high power microscopic field as follows: 12 (30%) lymph nodes with 1–4 immunoblasts; 14 (35%) lymph nodes with 5–15 immunoblasts;

and 14 (35%) lymph nodes with >15 immunoblasts (Fig. 2d). Immunoblasts did not form aggregates or sheets, were not located within sinusoids and were negative for CD15 and ALK1 in all cases tested. In the paracortical regions, Ki-67 showed a proliferative index of <15% in 31 (78%) lymph node and 15–30% in 9 (22%) lymph node samples; none of the lymph nodes tested showed a proliferative index >30%. In ten lymph node specimens tested, antibodies specific for CD11c and CD33 highlighted virtually all paracortical histiocytic cells. In addition, two of three samples tested for CD123 highlighted occasional loose clusters of plasmacytoid dendritic cells, which were predominately distributed in the deep paracortical areas, especially around blood vessels.

In the cortex, CD21 highlighted follicular dendritic cells and CD11c was positive in rare scattered dendritic cells associated with lymphoid follicles. Follicular dendritic cells were negative for all other markers tested including CD1a, langerin, S100 protein, CD68, CD163, E-cadherin, cyclin D1, and p-ERK.

In the subcapsular, trabecular, and medullary sinuses, CD163 highlighted macrophages, corresponding to 90–100% (median, 90%) of histiocytic cells within sinuses (Fig. 4e). Similarly, CD68 was positive in 90–100%

Table 2 Summary of histopathologic features of 50 lymph node samples from patients with dermatopathic lymphadenopathy, including comparison between cases associated and unassociated with mycosis fungoides.

	All cases (%)	MF (%)	Non-MF (%)	*P* value
Lymphadenopathy distribution (*n* = 42)				
Axillary	15/42 (36)	2/6 (33)	13/36 (36)	0.9999
Inguinal	6/42 (14)	0/6	6/36 (17)	0.5688
Axillary and inguinal	10/42 (24)	3/6 (50)	7/36 (19)	0.1349
Intramammary	3/42 (7)	0/6	3/36 (8)	0.9999
Cervical	3/42 (7)	0/6	3/36 (8)	0.9999
Multicompartmental	5/42 (12)	1/6 (17)	4/36 (12)	0.5378
Laterality				
Unilateral	19/42 (45)	1/6 (17)	18/36 (50)	0.1973
Bilateral	23/42 (55)	5/6 (83)	18/36 (50)	
Histopathologic features (*n* = 50)				
DL categories				0.0556
(1) Mild	13/50 (26)	1/9 (11)	12/41 (29)	
(2) Moderate	16/50 (32)	1/9 (11)	15/41 (37)	
(3) Severe	21/50 (42)	7/9 (78)	14/41 (34)	**0.0253***
Atypical (cerebriform) lymphocytes				
Present	35/50 (70)	8/9 (89)	27/41 (66)	0.2465
Absent	15/50 (30)	1/9 (11)	14/41 (34)	
NCI-VA classification**				
LN0	15/50 (30)	1/9 (11)	14/41 (34)	0.3760
LN1	19/50 (38)	4/9 (44.5)	15/41 (37)	
LN2	16/50 (32)	4/9 (44.5)	12/41 (29)	
LN3	0/50	0/9	0/41	
LN4	0/50	0/9	0/41	
Pigment-laden macrophages				0.2021
Absent	2/50 (4)	0/9	2/41 (5)	
Scant	11/50 (22)	1/9 (11)	10/41 (24)	
Moderate	18/50 (36)	6/9 (67)	12/41 (29)	
Abundant	19/50 (38)	2/9 (22)	17/41 (42)	
Lymph node paracortex				
Eosinophils[a]				
0	26/50 (52)	3/9 (33)	23/41 (56)	0.3851
1+	18/50 (36)	5/9 (56)	13/41 (32)	
2+	6/50 (12)	1/9 (11)	5/41 (12)	
3+	0/50	0/9	0/41	
Mitotic figures[a]				
0	11/50 (22)	1/9 (11)	10/41 (24)	0.6765
1+	30/50 (60)	6/9 (67)	24/41 (59)	
2+	9/50 (18)	2/9 (22)	7/41 (17)	
3+	0/50	0/9	0/41	
Immunoblasts[b]				
0	0/40	0/7	0/33	
1+	12/40 (30)	1/7 (14)	11/33 (33)	0.3702
2+	14/40 (35)	2/7 (29)	12/33 (37)	
3+	14/40 (35)	4/7 (57)	10/33 (30)	
Small thin-walled branching blood vessels				0.4251
Present	38/50 (76)	8/9 (89)	30/41 (73)	
Absent	12/50 (24)	1/9 (11)	11/41 (27)	
Immunophenotype of paracortical histiocytic cells				
S100 protein, median (range) (%)	90 (80–90)	90 (90–90)	90 (80–90)	0.1830
CD1a, median (range) (%)	80 (70–90)	90 (70–90)	80 (70–90)	0.6294
Langerin, median (range) (%)	35 (10–70)	10 (10–60)	30 (10–60)	0.0826
Lymph node cortex				
Castleman-like changes[c]				>0.9999

Table 2 (continued)

	All cases (%)	MF (%)	Non-MF (%)	P value
Present	18/50 (36)	3/9 (33)	15/41 (37)	
Absent	32/50 (64)	6/9 (67)	26/41 (63)	
Follicular hyperplasia				>0.9999
Present	29/50 (58)	5/9 (56)	24/41 (58)	
Absent	21/50 (42)	4/9 (44)	17/41 (42)	
Capsule and trabeculae				
Fibrosis				0.4255
Present	15/42 (36)	4/8 (50)	11/34 (33)	
Absent	27/42 (64)	4/8 (50)	23/34 (67)	

*Statistically significant *P* values

**In the presence of clinically abnormal lymph nodes, NCI-VA grades LN 0 to 2 correspond to nodal stage N1 according to the International Society for Cutaneous Lymphomas/European Organization for Research and Treatment of Cancer (ISCL/EORTC) staging system

aParacortical eosinophils and mitotic figures were quantified as the average number in ten high power fields (400×) and classified as: 0 (absent), 1+ (1–3 per high power field), 2+ (4–5 per high power field) and 3+ (>5 per high power field)

bImmunoblasts, defined as CD30-positive medium-sized lymphoid cells with visible nucleoli were quantified in the paracortex as the average in ten high power fields (400×) and reported as: 0 (absent), (+) 1–4, (2+) 5–15, and (3+) >15 immunoblasts per high power field

cCastleman-like changes were defined as the presence of three or more follicles with both regressive changes and onion skin-like mantle zones
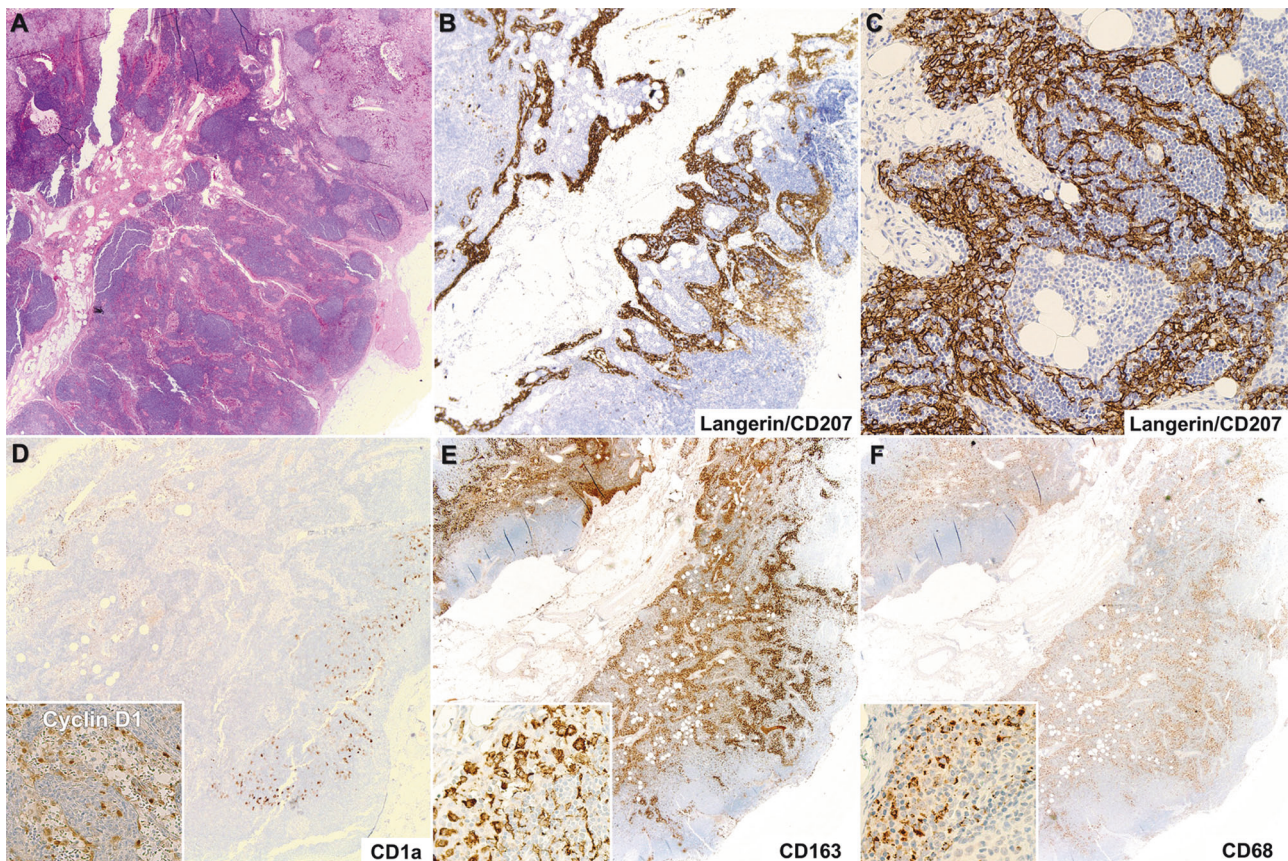

Fig. 4 Dermatopathic lymphadenopathy. a Partially involving a lymph node (Patient #25) showing patent sinuses and medullary cords (×20) **b, c** Langerin/CD207 shows a linear and reticular pattern of immunopositivity in cells of the lymph node conduit system including trabecular sinuses, medullary sinuses and cords (20×, 400×); **d** without coexpression CD1a (20×); or cyclin D1, which highlights the nuclei of sinus macrophages and endothelial cells (×200, inset). **e, f** Sinus macrophages are positive for CD163 (**e**) and CD68 (**f**) comprising ~90% of sinus histiocytic cells (×20, ×400 inset).

Table 3 Summary of the results of immunohistochemical analysis of histiocytic cells in lymph nodes with dermatopathic lymphadenopathy.

Marker	Paracortex		Sinuses	
	Positive cases over total cases tested (%)[a]	Percentage of histiocytic cells positive for the marker	Positive cases over total cases tested (%)[a]	Percentage of histiocytic cells positive for the marker
S100 protein[b]	50/50 (100)	80–90% (median, 90%)	0/50	NA
CD1a[c]	50/50 (100)	70–90% (median, 80%)	0/50	NA
Langerin/CD207	50/50 (100)	10–70% (median, 35%)	31/50 (62)	NA[d]
CD11c	10/10 (100)	100%	10/10 (100)	100%
CD33	10/10 (100)	100%	10/10 (100)	100%
CD68 (KP1)	40/40 (100)	10–25% (median, 15%)	40/40 (100)	90–100% (median, 90%)
CD163	40/40 (100)	10–25% (median, 15%)	40/40 (100)	90–100% (median, 90%)
E-cadherin	40/40 (100)	5–20% (median, 10%)	0/40	NA
BRAF V600E (VE-1)	0/40	NA	0/40	NA
Cyclin D1	40/40 (macrophages only)[e,f]	<10%	38/40 (95)[f]	5–25% in 20 (53%) 25–50% in 15 (39%) >50% in 3 (8%)
p-ERK	40/40 (macrophages only)[e]	<10%	0/40	NA

NA not applicable

[a]Cases were considered positive if staining was present in ≥5% of histiocytic cells

[b]In every case, the intensity of staining of S100 protein and langerin in the paracortical areas was strong and homogenous

[c]In each individual case, CD1a showed heterogeneous (weak, moderate, and strong) intensity of staining

[d]Langerin-positive cells in the sinuses of dermatopathic lymph nodes were arranged in meshworks delineating lymph node sinuses and did not display the typical morphology of sinus histiocytes. Therefore quantification in relation to the total number of sinus histiocytic cells was not performed

[e]Although in paracortical lymph node areas cyclin D1 and p-ERK were negative in dendritic cells, these markers were expressed in the nucleus of rare (<10%) paracortical macrophages

[f]In each individual case, the intensity of cyclin D1 expression was heterogeneous, varying from weak to moderate

(median, 90%) of histiocytic cells within sinuses in all lymph nodes examined (Fig. 4f). CD11c was positive in virtually all histiocytic cells within sinuses. Cyclin D1 highlighted the nuclei of sinus histiocytic cells in 38 (95%) of 40 lymph nodes examined; specifically, 5–25% of the sinus histiocytic cells in 20 (53%) lymph node samples, 25–50% of the sinus histiocytic cells in 15 (39%), and in >50% of sinus histiocytic cells in 3 (8%) samples assessed. Notably, the intensity of cyclin D1 expression was broadly heterogeneous among individual cells, varying from weak to moderate. (Fig. 4d, inset) Unexpectedly, langerin was expressed by cells in the sinuses and medullary cords of 31 (62%) of 50 lymph nodes examined, showing moderate to strong staining intensity. Furthermore, in every positive case, langerin-positive cells were organized into tight linear meshworks delineating the walls of the lymph node sinuses and medullary cords, instead of showing the typical morphology and distribution of sinus histiocytes (Fig. 4b, c). In 25 (81%) of 31 lymph nodes, langerin-positive cells were present in the trabecular sinuses, medullary sinuses and cords; and in 6 (19%) samples langerin-positive cells were additionally found in the subcapsular sinuses. Notably, these langerin-positive cells were negative for CD1a (Fig. 4d). Cyclin D1 (Fig. 4f, inset) and fibroblastic reticular cell markers such as desmin, smooth muscle actin, and vimentin failed to reveal a staining pattern similar to that shown by langerin. S100 protein, E-cadherin, and p-ERK highlighted <5% of histiocytic cells within sinuses. A summary of the results of the immunohistochemical analysis of histiocytic cells in lymph nodes with dermatopathic lymphadenopathy is provided in Table 3.

The immunophenotype of B cells, T cells, and plasma cells was assessed by flow cytometry in 24 lymph node samples, including those from patients with clinical history B- or T-cell lymphoma. B-cells and plasma cells were polytypic in all samples. Among a total of six lymph node samples from six patients with mycosis fungoides that were analyzed by flow cytometry, two (patients #25 and #39) showed aberrant T-cell populations, which comprised ~10% and 15% of the total lymphocyte population, respectively. The remaining, 22 lymph node samples tested did not show aberrant expression of T-cell antigens.

Comparison between dermatopathic lymphadenopathy associated and unassociated with mycosis fungoides

We compared key clinicopathologic and immunophenotypic features of dermatopathic lymphadenopathy arising in the setting of mycosis fungoides with cases not associated with mycosis fungoides (Table 2). Lymph node samples from patients with mycosis fungoides showed florid (category 3) dermatopathic changes significantly more often than lymph nodes from patients without associated mycosis fungoides (78 vs. 34%, $p = 0.0253$). Conversely, the latter group displayed the full spectrum of dermatopathic changes ranging from mild to severe. Notably, lymph node specimens from patients with and without mycosis fungoides showed atypical lymphocytes with cerebriform or hyperconvoluted nuclei (89% vs. 66%, $p = 0.2465$), corresponding to stages LN0 to LN2 when classified according to the National Cancer Institute-Veterans Administration Hospital system (NCI-VA) and stage N1 according to the ISCL/EORTC classification. As defined by our inclusion criteria, none of the lymph node samples showed partial or complete architectural effacement by atypical cerebriform lymphocytes that would be consistent with stages LN3 or LN4 NCI, or N2 or N3 (ISCL/EORTC). No other clinicopathologic or immunophenotypic differences were observed between the two subgroups. A summary of key clinicopathologic and immunophenotypic features, including a comparison between cases of dermatopathic lymphadenopathy associated and unassociated with mycosis fungoides is provided in Table 2.

Molecular results

As stated above, the 146-gene panel included genes shown previously to be relevant to the pathogenesis of histiocytic disorders such as *ARAF*, *BRAF*, *CCND1*, *ERBB1*, *ERBB2*, *ERBB3*, *KRAS*, *MAP2K1*, *NRAS*, *PIK3CA*, *SRC*, and *SMAD4*. No gene mutations were detected in five patients with available DNA from lymph node biopsy samples. Assessment of clonality revealed monoclonal *TRG* and *TRB* rearrangements in two (20%) of ten samples, both from patients with mycosis fungoides (patient #25 and #39). The other eight lymph node samples tested, including four samples of dermatopathic lymphadenopathy occurring in the setting of mycosis fungoides, showed a polyclonal pattern of *TRG* and *TRB* rearrangements.

Discussion

Dermatopathic lymphadenopathy is a distinctive lymph node reaction pattern that typically occurs in patients with cutaneous diseases. Other than case reports, most studies on dermatopathic lymphadenopathy were published over two decades ago when there were relatively few antibodies available and, as a result, detailed immunophenotypic studies of dermatopathic lymphadenopathy are few. In this study, we present an update on the clinicopathologic features of dermatopathic lymphadenopathy with a special focus on the immunophenotype and distribution of histiocytic cells (i.e., dendritic cells, macrophages, and others) in the different compartments of dermatopathic lymph nodes.

All lymph node specimens in this study showed typical histopathologic features of dermatopathic lymphadenopathy, including paracortical areas expanded by varying numbers of pale-staining dendritic cells and lymphocytes. Immunohistochemical analysis, however, yielded results that are somewhat different from those previously reported in the literature [2, 24]. In all cases, we observed that S100 protein and CD1a were expressed by paracortical dendritic cells to a very similar extent and distribution. However, whereas S100 protein consistently showed strong, homogeneous reactivity, the intensity of CD1a among individual paracortical dendritic cells was heterogeneous, including dendritic cells with strong/high expression of CD1a, closely intermingled with other dendritic cells with weak/low intensity of expression of CD1a. Another finding of note is that the number of CD1a-positive cells in the paracortical areas was significantly higher than the number of langerin expressing cells.

These findings are better understood in light of recent advances in the characterization and classification of human dendritic cell subsets [6, 7, 25]. Dendritic cells are bone marrow-derived members of the mononuclear phagocyte system found in the circulation, lymphoid tissues, and other organs including the spleen, liver, skin, lungs, and intestines [6, 7]. Dendritic cells constitute the most efficient translators between the innate and adaptive immune system due to their capacity to capture, process, and present antigens on major histocompatibility complex molecules and activate naïve T-cells [6, 7, 26–29]. A recently proposed unified classification identifies three main types of human dendritic cell subsets: plasmacytoid dendritic cells and myeloid ("classical") dendritic cells, types 1 and 2. Plasmacytoid dendritic cells have eccentric nuclei, prominent endoplasmic reticulum, and a Golgi complex to produce type I and type III interferon; these cells express CD123 (interleukin-3 receptor), CD303 (BDCA-2; blood dendritic cell antigen 2), and CD304 (BDCA-4), and do not express CD11c or the myeloid antigens CD13 and CD33. Type 2 myeloid dendritic cells represent the major population of myeloid dendritic cells in blood and lymphoid and nonlymphoid organs; most interdigitating dendritic cells in the T-cell areas in lymph nodes correspond to type 2 myeloid dendritic cells [6]. Type 1 myeloid dendritic cells are found at one-tenth the frequency of type 2 dendritic cells in steady-state blood, among resident dendritic cells of lymph nodes and other

tissues. Immunophenotypically, while both type 1 and type 2 myeloid dendritic cells express CD13 and CD33, only type 2 myeloid dendritic cells show CD1a expression, which is characteristically low/dim [6, 7, 29]. Other markers frequently used by experimental immunologists to distinguish type 1 from type 2 include CD1c (BDCA-1), CD11b, and CD172a (SIRP alpha; signal-regulatory protein alpha) which are expressed by type 2 but not type 1 myeloid dendritic cells; and CD141 (BDCA-3) which is expressed by type 1 myeloid dendritic cells [6, 25]. In a separate category are Langerhans cells, which are specialized self-renewing dendritic cells that share a primitive origin with brain microglia and other tissue macrophages, as they originate from yolk sac-derived myeloid progenitors and fetal liver monocytes (embryonic derived) [6, 7, 26]. Immunophenotypically, Langerhans cells can be distinguished from type 2 myeloid dendritic cells by their high expression of the C-type lectin langerin, an endocytic receptor that induces the formation of Birbeck granules; and by higher/brighter expression of CD1a [6, 7, 26–29]. Table 4

summarizes the major mononuclear phagocyte (histiocyte) categories and their immunophenotype.

Taken together, these data and the findings we present suggest that the paracortical regions of dermatopathic lymph nodes harbor, at minimum, three immunophenotypically distinct subsets of dendritic cells. These subsets include: Langerhans cells (S100+, CD1a$^{+(high)}$, langerin$^{+(high)}$); interdigitating dendritic cells, which likely consists of type 2 myeloid dendritic cells (S100+, CD1a+$^{(low)}$, langerin-); and, at least, a third minor population of S100 protein-positive dendritic cells that do not express CD1a and langerin, possibly corresponding to type 1 myeloid dendritic cells [6, 30]. These findings add information to the usual simplified description of dermatopathic lymph nodes as harboring only two types of dendritic cells in the paracortex (i.e., interdigitating dendritic cells and Langerhans cells). Furthermore, our findings show that CD1a is not expressed exclusively by Langerhans cells, but also by other dendritic cell subsets in dermatopathic lymph nodes. Others have described the immunophenotypic heterogeneity of dendritic-cell

Table 4 Major mononuclear phagocyte (histiocyte) categories and their immunophenotype [6, 8, 25, 41, 56, 57].

| Marker | Plasmacytoid dendritic cells | Langerhans cells | Myeloid or "classical" dendritic cells | | Macrophages[b] | | Monocytes |
			Type 1	Type 2	M1	M2	
CD1a	–	+ HIGH	–	+ LOW	–	–	–
CD1c/BCDA-1	–	+	–	+	NA	NA	+/–
CD11b	–	+	–	+	+	+	+
CD11c	–	+ LOW	+ LOW	+ HIGH	+	+	+
CD13	–	+	+	+	+	+	+
CD14	–	–	–	–	+	+	+
CD33	–	+	+	+	+	+	+
CD68 (KP1)	+	+	NA	NA	+	+	+
CD68 (PG-M1)	+	+/–	NA	NA	+	+	+
CD123/IL3α	+	–	–	–	-	-	-
CD141/BDCA-3	–	–	+	–	NA	NA	+
CD163	–	–	–	–	-	+	+
CD172a/SIRPα	–	+	–	+	+	+	+
CD207/Langerin	–	+ HIGH	–	–[a]	–	–	–
CD303/BDCA-2	+	–	–	–	–	–	–
CD304/BDCA-4	+	–	–	–	NA	NA	NA
Birbeck granules	–	+	–	–	–	–	–
E-cadherin	–	+	–	–	–	–	–
EpCAM	–	+	–	–	–	–	–

BCDA-1 blood-derived circulating antigen-1, *BCDA-2* blood-derived circulating antigen-2, *BCDA-3* blood-derived circulating antigen-3, *BCDA-4* blood-derived circulating antigen-4, *EpCAM* epithelial cell adhesion molecule, *IL3α* interleukin-3 receptor alpha, *NA* not available, *SIRPα* signall regulatory protein alpha

[a]In myeloid dendritic cells type 2, langerin has been detected at low levels in vivo, and at high levels in vitro in response to transforming growth factor-beta stimulation

[b]M1 (classically activated) and M2 (alternatively activated) denote the two major functional categories of macrophages
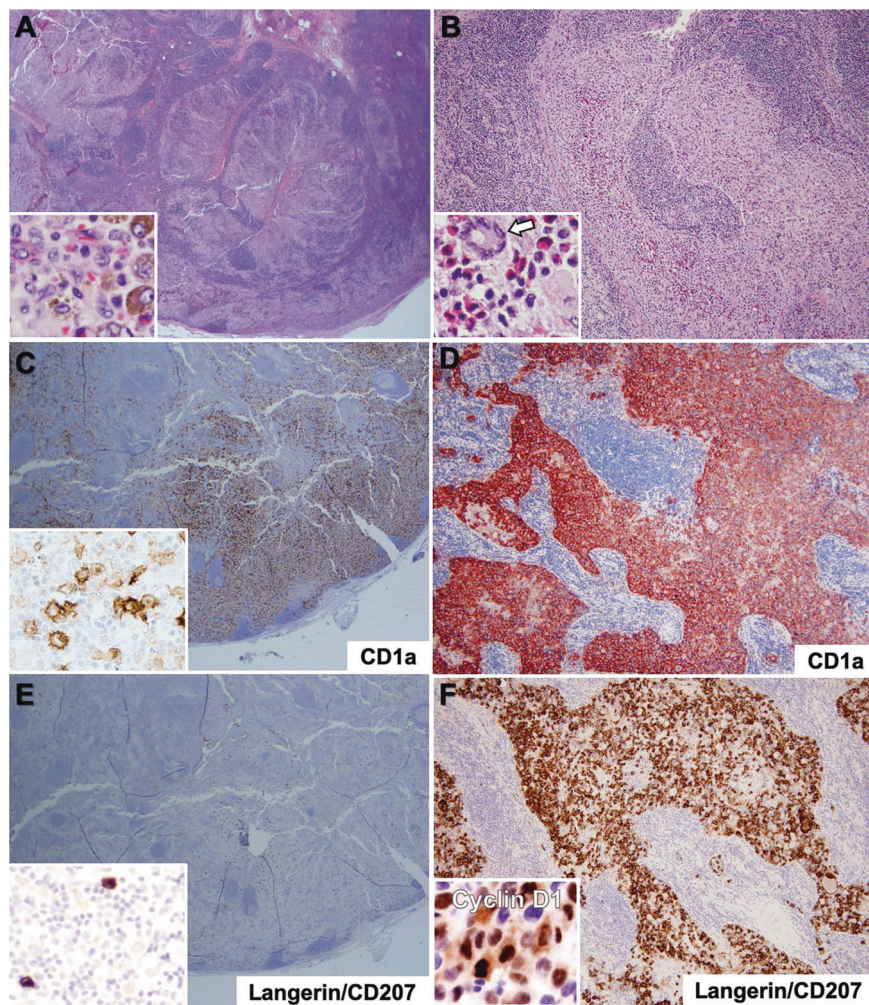
Fig. 5 Comparison of pathologic and immunophenotypic findings between dermatopathic lymphadenopathy and Langerhans cell histiocytosis involving lymph nodes. a A case of florid (category 3) dermatopathic lymphadenopathy (case 4) with massive expansion of the lymph node paracortex by nodular, pale-staining areas composed of Langerhans cells and other dendritic cells (20×). The inset shows dendritic cells with delicately folded nuclei, pigment-laden macrophages and occasional eosinophils (1000×). **b** A case of Langerhans cell histiocytosis involving lymph node in a predominantly sinus pattern (100×). The inset shows neoplastic Langerhans cells admixed with giant cells (arrow) and many eosinophils, frequently forming "eosinophilic abscesses" (1000×). **c** In the case of dermatopathic lymphadenopathy, ~90% of the histiocytic cells expanding paracortical areas are positive for CD1a, which shows variable intensity (20×; 400× inset), **d** and in the case of Langerhans cell histiocytosis CD1a shows diffuse strong expression by neoplastic Langerhans cells within the lymph node sinuses (100×) **e** Langerin in dermatopathic lymphadenopathy is positive in ~5% of histiocytic cells in the paracortex (100×; 400× inset). Cyclin D1 was negative in the paracortical areas of this lymph node (not shown). **f** Conversely, in the case of Langerhans cell histiocytosis, there is diffuse and strong staining of >90% of the neoplastic Langerhans cells within sinuses (200×). The neoplastic Langerhans cells were also positive for cyclin D1 showing strong nuclear and moderate cytoplasmic expression (400×, inset).

populations colonizing the paracortex of skin-draining lymph nodes [5, 8, 9]. Angel et al. using dual-color immunofluorescence-based methods examined antigen-presenting cell-populations inhabiting the paracortex of histologically normal or "mildly reactive" axillary (i.e. skin-draining) lymph nodes and found colonization by at least three immunophenotypically distinct antigen-presenting cell subsets, including two distinct subsets that expressed CD1a with and without coexpression of langerin, respectively; and a third subset that was negative for both markers. Comparable with our findings, in their study only ~20–50% of

CD1a-positive cells expressed langerin [5]. The antigenic heterogeneity of dendritic-cell populations colonizing the paracortex of skin-draining lymph nodes might reflect not only the presence of multiple distinct dendritic cell subsets, but also the varying stages of activation of these cells [5, 6, 8, 9]. Additional multiparameter immunophenotypic studies are needed to fully characterize the different dendritic cell subsets colonizing dermatopathic lymph nodes.

Another finding of interest is the presence of langerin-positive cells arranged in meshworks that appear to delineate lymph node sinuses and medullary cords in more

than 60% of dermatopathic lymph nodes. These cells do not have the morphology of Langerhans cells or sinus macrophages and are negative for other histiocytic markers, as well as for fibroblastic reticular cell markers [31]. Comparable results were obtained by Chikwava and Jaffe in a study analyzing the immunohistochemical expression of langerin in various types of pediatric tissue samples. They described langerin immunostaining without coexpression of CD1a in "fixed tissue elements" in the sinuses of all 12 dermatopathic lymph nodes, and other reactive lymph nodes analyzed. Notably, Chikwava and Jaffe used the same type of anti-langerin antibody (Novocastra, clone 12D6) used in the current study [32]. Considering the striking linear and reticular pattern of immunopositivity, these cells may truly express langerin. An alternative explanation, however, is that the anti-langerin antibody is cross-reacting with related lectin-type molecules present in histiocytic or structural cells of lymph node sinuses, for instance, sinus-lining cells of lymph nodes. Sinus-lining cells, considered by some to be variants of fibroblastic reticular cells, are immune accessory cells with dendritic morphology that exhibit endothelial and histiocytic structural and functional properties. These cells are organized in flattened cellular networks that line lymph node sinuses, where they are thought to filter and trap antigens [33–37]. An older study of sinus-lining cells of lymph nodes illustrated a strikingly similar pattern of immunostaining with the monoclonal antibody Ki-M9 and reported that these cells, similar to our results, were not labeled by CD11c, CD68, CD1a, or S100 protein [36]. Other possibilities include cross-reactivity with non-langerin molecules present in sinus macrophages, although this possibility seems less likely due to the dissimilar pattern of staining observed in langerin compared with CD163.

Functionally, macrophages are broadly categorized into two types: M1 and M2; this nomenclature is derived from the T-helper type 1 and type 2 immune responses promoted by the two types of macrophages, respectively [37]. In this study, the predominant phenotype of macrophages in dermatopathic lymph nodes was CD68+/CD163+, which has been generally accepted as an M2-like macrophage phenotype [37–40]. Recent immunohistochemistry-based studies, however, advocate the addition of transcription factor markers, including STAT1 and RBP-J for M1, and C-MAF for M2, as a better approach to determine the polarization status in tissue infiltrating macrophages [41] Moreover, it has been increasingly recognized that the M1/M2 classification is an oversimplified approach that describes two extreme phenotypes that are part of a continuum of phenotypic changes that occur during macrophage activation [42]. Therefore, although it is tempting to propose that macrophages in dermatopathic lymph nodes show mostly M2 polarization, additional studies are needed to more specifically categorize the macrophage populations colonizing the different

compartments of dermatopathic lymph nodes and their functional properties (Table 4).

Another notable finding is the strikingly high number of CD30-positive intermediate-sized immunoblasts scattered in the paracortical regions of more than half of dermatopathic lymph nodes. The marked increase in CD30-positive cells might raise the differential diagnosis of lymphoma, in particular, classic Hodgkin lymphoma or variants of non-Hodgkin lymphoma associated with many histiocytes (e.g., lymphohistiocytic variant of anaplastic large cell lymphoma). In the present study, however, increased immunoblasts were usually evenly dispersed in the paracortex, did not form clusters of more than three cells, were not present within lymph node sinusoids, and were negative for CD15 and ALK1.

Although not the focus of this study, a well-known diagnostic challenge is the differential diagnosis of dermatopathic lymphadenopathy and mycosis fungoides/Sézary Syndrome [15, 18, 19, 43–47]. In this study group, irrespective of the nature of the underlying disease, we identified atypical lymphocytes with cerebriform nuclei in ~70% of lymph nodes, including 28 (68%) from patients without mycosis fungoides; and 7 (75%) from patients with mycosis fungoides. These morphologic changes would be classified as stages LN1–2 (NCI-VA), or as stage N1 (ISCL/EORTC). Also, when comparing other morphologic parameters in dermatopathic lymph nodes arising in these two clinical settings, the only significant difference was a higher frequency of severe or florid (category 3) dermatopathic changes in lymph nodes from patients with mycosis fungoides. The lack of clear-cut morphologic features to distinguish these two entities has been long acknowledged [15, 18, 45]. In 1981, Burke et al. reported more extensive dermatopathic changes among lymph nodes associated with mycosis fungoides than in lymph nodes not associated with mycosis fungoides; nevertheless, no other morphologic features were exclusive for either group, including the quantity and distribution of atypical cerebriform lymphocytes [18]. Currently, highly sensitive multicolor flow cytometry and molecular studies to assess for T-cell clonality are often used for the detection of potential low-level involvement of dermatopathic lymph nodes by mycosis fungoides/Sezary syndrome [23, 47].

One more important histologic differential diagnosis to consider is Langerhans cell histiocytosis involving lymph nodes. Langerhans cell histiocytosis most often occurs in pediatric patients and rarely occurs primarily in lymph nodes [48, 49]. Cervical lymph nodes are most often involved, in up to 80% of cases, and axillary or inguinal are involved uncommonly [49, 50] By contrast, dermatopathic lymphadenopathy most commonly involves axillary and inguinal lymph nodes and rarely cervical lymph nodes. There are also histopathologic and immunoarchitectural differences between these two entities. Langerhans cell

histiocytosis commonly involves lymph node sinuses, either extensively or focally, in addition to nodal paracortical areas [48, 49]. In contrast, dermatopathic lymphadenopathy is a paracortical process. Sinus histiocytosis is also present in dermatopathic lymph nodes; however, CD1a-positive and S100 protein-positive dendritic cells represent <5% of histiocytic cells within sinuses. Importantly though, while a sinus pattern of involvement supports Langerhans cell histiocytosis, in some cases with extensive disease, the neoplastic Langerhans cells can infiltrate the paracortex and obscure the characteristic sinus pattern [48]. Moreover, as previously reported in one study, and seen in more than half of dermatopathic lymph nodes in the current study group, the anti-langerin antibody clone 12D6 from Novocastra may show striking positivity in cells that delineate lymph node sinuses and medullary cords [32]. It is advisable to become familiar with this distinctive pattern of langerin staining, which will not be accompanied by coexpression of other dendritic cell makers, including CD1a and S100 protein. Other helpful morphologic differences supporting Langerhans cell histiocytosis involving lymph nodes include: necrosis, present in up to 50% of cases of nodal Langerhans cell histiocytosis and absent in all cases of dermatopathic lymphadenopathy; eosinophils, abundant in more than half of cases of nodal Langerhans cell histiocytosis and absent or present only in low to moderate numbers in cases of dermatopathic lymphadenopathy; plasma cells, present in only 10% of cases of Langerhans cell histiocytosis and in 100% of cases of dermatopathic lymphadenopathy; and giant cells, present in 45% of cases of cases of Langerhans cell histiocytosis and absent in all cases of dermatopathic lymphadenopathy [48]. Lastly, none of the cases of dermatopathic lymphadenopathy showed expression of BRAF V600E (VE-1), cyclin D1, or p-ERK by dendritic cells in the paracortex, nor did we identify MAPK/ERK pathway-related gene mutations, unlike Langerhans cell histiocytosis, as has been shown by others [50–53]. Some of these differences are illustrated in Fig. 5, which compares a case of Langerhans cell histiocytosis from our archives with a case of dermatopathic lymphadenopathy.

Clinically, whereas dermatopathic lymphadenopathy is best known as occurring in patients with skin disease, this lymph node reaction pattern also has been described in patients without skin disease [16, 54]. Accordingly, almost half of the patients in this study did not have dermatologic signs or symptoms prior to or at the time at which lymphadenopathy was detected. Gould et al. studied lymph nodes from 50 axillary dissections of patients with breast cancer, without skin disease, and observed mild to moderate dermatopathic changes in 22% of lymph nodes that were not enlarged; they concluded that the findings might represent "the end of a histologic spectrum present in axillary lymph nodes." [16] In a more recent study, Angel et al. detected colonization of antigen-presenting cells including Langerhans cells in the paracortex of axillary and inguinal, but not in hilar and cervical lymph nodes of patients without skin disorders [5]. The explanation for axillary and inguinal lymph nodes being colonized may be attributable to their drainage of large areas of the skin [55]. The above findings have led to the theory that even under "steady-state" (i.e. not overt inflammatory) conditions, dermal dendritic cells continuously migrate to regional lymph node T-cell areas where they cooperate to regulate immune responses [5]. Therefore, in cases where lymph nodes are not clinically enlarged, and the detection of somewhat expanded paracortical dendritic cells is merely incidental, we believe that a diagnosis of paracortical hyperplasia may be more suitable. For this study, with the goal of offering guidance for distinguishing between mild dermatopathic lymphadenopathy and paracortical hyperplasia, our minimum criterion to define dermatopathic lymphadenopathy required dendritic cells (i.e., Langerhans cells and others) to be arranged in confluent collections of at least 20 dendritic cells.

In summary, we provide an update on the definition, clinicopathologic and immunoarchitectural features of dermatopathic lymphadenopathy. Our findings suggest that the paracortical regions of dermatopathic lymph nodes harbor heterogeneous populations of dendritic cells expressing varying combinations of S100 protein, CD1a, and langerin. We also show that cases of dermatopathic lymphadenopathy lack genetic mutations or aberrant activation of components of the MAPK/ERK pathway. Lastly, we summarize potential pitfalls and common and distinguishing features between dermatopathic lymphadenopathy and other entities involving lymph nodes in the differential diagnosis, including mycosis fungoides and Langerhans cell histiocytosis.

Compliance with ethical standards

References

1. Hurwitt E. Dermatopathic lymphadenitis: Focal granulomatous lymphadenitis associated with chronic generalized skin disorder. J Investig Dermatol. 1942;5:197–204.
2. Ioachim HL, Medeiros LJ. Dermatopathic lymphadenopathy. In: Ioachim HL Medeiros LJ, editors. Ioachim's lymph node pathology. Fourth edition. Philadelphia, PA: Lippincott Williams & Wilkins, 2009. p. 223–6.
3. Pautrier LM, Woringer F. Contribution a l'étude de l'histo-physiologie cutanée: a propos d'un aspect histo-pathologique nouveau

du ganglion lymphatique: réticulose lipo-mélanique accompagnant certainesdermatoses généralisées. Les échanges entre la peau et le ganglion. Ann Dermatol Syphiligr. 1937;8:257–73.

4. Steffen C. Frederic Woringer: Pautrier-Woringer disease (lipomelanotic reticulosis/dermatopathic lymphadenitis). Am J Dermatopathol. 2004;26:499–503.

5. Angel CE, Chen CJ, Horlacher OC, Winkler S, John T, Browning J, et al. Distinctive localization of antigen-presenting cells in human lymph nodes. Blood. 2009;113:1257–67.

6. Collin M, Bigley V. Human dendritic cell subsets: an update. Immunology. 2018;154:3–20.

7. Collin M, McGovern N, Haniffa M. Human dendritic cell subsets. Immunology. 2013;140:22–30.

8. Geissmann F, Dieu-Nosjean MC, Dezutter C, Valladeau J, Kayal S, Leborgne M, et al. Accumulation of immature Langerhans cells in human lymph nodes draining chronically inflamed skin. J Exp Med. 2002;196:417–30.

9. Segura E, Valladeau-Guilemond J, Donnadieu MH, Sastre-Garau X, Soumelis V, Amigorena S, et al. Characterization of resident and migratory dendritic cells in human lymph nodes. J Exp Med. 2012;209:653–60.

10. Rausch E, Kaiserling E, Goos M. Langerhans cells and interdigitating reticulum cells in the thymus-dependent region in human dermatopathic lymphadenitis. Virchows Arch B Cell Pathol. 1977;25:327–43.

11. Ackerman AB. Coming to specific diagnosis by another route: "onspecific findings as vehicle". In: Ackerman AB, Boer A, Bennin B, Gottlieb GJ, editors. Histologic diagnosis of inflammatory skin diseases: an algorithmic method based on pattern analysis. Third edition. United States of America: Ardor Scribendi, Ltd.; 2005. p. 417.

12. Hemmi H, Yoshino M, Yamazaki H, Naito M, Iyoda T, Omatsu Y, et al. Skin antigens in the steady state are trafficked to regional lymph nodes by transforming growth factor-beta1-dependent cells. Int Immunol. 2001;13:695–704.

13. Jimbow K, Sato S, Kukita A. Cells containing Langerhans granules in human lymph nodes of dermatopathic lymphadenopathy. J Investig Dermatol. 1969;53:295–9.

14. Lampert IA, Pizzolo G, Thomas A, Janossy G. Immunohistochemical characterization of cells involved in dermatopathic lymphadenopathy. J Pathol. 1980;131:145–56.

15. Burke JS, Sheibani K, Rappaport H. Dermatopathic lymphadenopathy. An immunophenotypic comparison of cases associated and unassociated with mycosis fungoides. Am J Pathol. 1986;123:256–63.

16. Gould E, Porto R, Albores-Saavedra J, Ibe MJ. Dermatopathic lymphadenitis. The spectrum and significance of its morphologic features. Arch Pathol Lab Med. 1988;112:1145–50.

17. Kojima M, Nakamura S, Itoh H, Yamane Y, Shimizu K, Murayama K, et al. Clinical implication of dermatopathic lymphadenopathy among Japanese: a report of 19 cases. Int J Surg Pathol. 2004;12:127–32.

18. Burke JS, Colby TV. Dermatopathic lymphadenopathy. Comparison of cases associated and unassociated with mycosis fungoides. Am J Surg Pathol. 1981;5:343–52.

19. Olsen E, Vonderheid E, Pimpinelli N, Willemze R, Kim Y, Knobler R, et al. Revisions to the staging and classification of mycosis fungoides and Sezary syndrome: a proposal of the International Society for Cutaneous Lymphomas (ISCL) and the cutaneous lymphoma task force of the European Organization of Research and Treatment of Cancer (EORTC). Blood. 2007;110:1713–22.

20. Khoury JD, Wang WL, Prieto VG, Medeiros LJ, Kalhor N, Hameed M, et al. Validation of immunohistochemical assays for integral biomarkers in the NCI-MATCH EAY13. Clinical trial. Clin Cancer Res. 2018;24:521–31.

21. Vrotsos E, Alexis J. Can SOX-10 or KBA.62 replace S100 protein in immunohistochemical evaluation of sentinel lymph nodes for metastatic melanoma? Appl Immunohistochem Mol Morphol. 2016;24:26–9.

22. Yabe M, Medeiros LJ, Tang G, Wang SA, Ahmed S, Nieto Y, et al. Prognostic factors of hepatosplenic T-cell lymphoma (HSTCL): a clinicopathologic, immunophenotypic, and cytogenetic analysis of 28 patients. Am J Surg Pathol. 2016;40:676–88.

23. Vega F, Medeiros LJ, Jones D, Abruzzo LV, Lai R, Manning J, et al. A novel four-color PCR assay to assess T-cell receptor gamma gene rearrangements in lymphoproliferative lesions. Am J Clin Pathol. 2001;116:17–24.

24. Garces S, Medeiros LJ, Patel KP, Li S, Pina-Oviedo S, Li J, et al. Mutually exclusive recurrent KRAS and MAP2K1 mutations in Rosai-Dorfman disease. Mod Pathol. 2017;30:1367–77.

25. Guilliams M, Ginhoux F, Jakubzick C, Naik SH, Onai N, Schraml BU, et al. Dendritic cells, monocytes and macrophages: a unified nomenclature based on ontogeny. Nat Rev Immunol. 2014;14:571–8.

26. Hoeffel G, Wang Y, Greter M, See P, Teo P, Malleret B, et al. Adult Langerhans cells derive predominantly from embryonic fetal liver monocytes with a minor contribution of yolk sac-derived macrophages. J Exp Med. 2012;209:1167–81.

27. Trinchieri G. Pillars of immunology: the birth of a cell type. J Immunol. 2007;178:3–4.

28. Steinman RM, Cohn ZA. Pillars article: identification of a novel cell type in peripheral lymphoid organs of mice. I. Morphology, quantitation, tissue distribution. J Exp Med. 1973;137:1142–62. J Immunol. 2007;178:5–25

29. Heidkamp GF, Sander J, Lehmann CHK, Heger L, Eissing N, Baranska A, et al. Human lymphoid organ dendritic cell identity is predominantly dictated by ontogeny, not tissue microenvironment. Sci Immunol. 2016;1:1–17.

30. Eisenbarth SC. Dendritic cell subsets in T cell programming: location dictates function. Nat Rev Immunol. 2019;19:89–103.

31. Fletcher AL, Acton SE, Knoblich K. Lymph node fibroblastic reticular cells in health and disease. Nat Rev Immunol. 2015;15:350–61.

32. Chikwava K, Jaffe R. Langerin (CD207) staining in normal pediatric tissues, reactive lymph nodes, and childhood histiocytic disorders. Pediatr Dev Pathol. 2004;7:607–14.

33. Willard-Mack CL. Normal structure, function, and histology of lymph nodes. Toxicol Pathol. 2006;34:409–24.

34. Krokowski M, Merz H, Thorns C, Bernd HW, Schade U, Le Tourneau A, et al. Sarcoma of follicular dendritic cells with features of sinus lining cells—a new subtype of reticulum cell sarcoma? Virchows Arch. 2008;452:565–70.

35. Wacker HH, Heidebrecht HJ, Radzun HJ, Parwaresch MR. Sinus lining cells: morphology, function and neoplasia. Verh Dtsch Ges Pathol. 1992;76:219–25.

36. Wacker HH, Frahm SO, Heidebrecht HJ, Parwaresch R. Sinus-lining cells of the lymph nodes recognized as a dendritic cell type by the new monoclonal antibody Ki-M9. Am J Pathol. 1997;151:423–34.

37. Mills CD, Kincaid K, Alt JM, Heilman MJ, Hill AM. M-1/M-2 macrophages and the Th1/Th2 paradigm. J Immunol. 2000;164:6166–73.

38. Lan C, Huang X, Lin S, Huang H, Cai Q, Wan T, et al. Expression of M2-polarized macrophages is associated with poor prognosis for advanced epithelial ovarian cancer. Technol Cancer Res Treat. 2013;12:259–67.

39. Khramtsova G, Liao C, Khramtsov A, Li S, Gong C, Huo D, et al. The M2/alternatively activated macrophage phenotype correlates with aggressive histopathologic features and poor clinical outcome in early stage breast cancer. Cancer Res. 2009;69:107.

40. Poles WA, Nishi EE, de Oliveira MB, Eugênio AIP, de Andrade TA, Campos AHFM, et al. Targeting the polarization of tumor-associated macrophages and modulating mir-155 expression might be a new approach to treat diffuse large B-cell lymphoma of the elderly. Cancer Immunol Immunother. 2019;68:269–82.

41. Barros MH, Hauck F, Dreyer JH, Kempkes B, Niedobitek G. Macrophage polarisation: an immunohistochemical approach for identifying M1 and M2 macrophages. PLoS ONE. 2013;8:e80908.

42. Ruytinx P, Proost P, Van Damme J, Struyf S. Chemokine-induced macrophage polarization in inflammatory conditions. Front Immunol. 2018;9:1930.

43. Cooper RA, Dawson PJ, Rambo ON. Dermatopathic lymphadenopathy a clinicopathologic analysis of lymph node biopsy over a fifteen-year period. Calif Med. 1967;106:170–5.

44. Colby TV, Burke JS, Hoppe RT. Lymph node biopsy in mycosis fungoides. Cancer. 1981;47:351–9.

45. Rappaport H, Thomas LB. Mycosis fungoides: the pathology of extracutaneous involvement. Cancer. 1974;34:1198–229.

46. Sausville EA, Worsham GF, Matthews MJ, Makuch RW, Fischmann AB, Schechter GP, et al. Histologic assessment of lymph nodes in mycosis fungoides/Sezary syndrome (cutaneous T-cell lymphoma): clinical correlations and prognostic import of a new classification system. Hum Pathol. 1985;16:1098–109.

47. Weiss LM, Hu E, Wood GS, Moulds C, Cleary ML, Warnke R, et al. Clonal rearrangements of T-cell receptor genes in mycosis fungoides and dermatopathic lymphadenopathy. N Engl J Med. 1985;313:539–44.

48. Edelweiss M, Medeiros LJ, Suster S, Moran CA. Lymph node involvement by Langerhans cell histiocytosis: a clinicopathologic and immunohistochemical study of 20 cases. Hum Pathol. 2007;38:1463–9.

49. Kakkar S, Kapila K, Verma K. Langerhans cell histiocytosis in lymph nodes. Cytomorphologic diagnosis and pitfalls. Acta Cytol. 2001;45:327–32.

50. Alayed K, Medeiros LJ, Patel KP, Zuo Z, Li S, Verma S, et al. BRAF and MAP2K1 mutations in Langerhans cell histiocytosis: a study of 50 cases. Hum Pathol. 2016;52:61–7.

51. Shanmugam V, Craig JW, Hornick JL, Morgan EA, Pinkus GS, Pozdnyakova O. Cyclin D1 is expressed in neoplastic cells of langerhans cell histiocytosis but not reactive langerhans cell proliferations. Am J Surg Pathol. 2017;41:1390–6.

52. Badalian-Very G, Vergilio JA, Degar BA, MacConaill LE, Brandner B, Calicchio ML, et al. Recurrent BRAF mutations in Langerhans cell histiocytosis. Blood. 2010;116:1919–23.

53. Brown NA, Furtado LV, Betz BL, Kiel MJ, Weigelin HC, Lim MS, et al. High prevalence of somatic MAP2K1 mutations in BRAF V600E-negative Langerhans cell histiocytosis. Blood. 2014;124:1655–8.

54. Vanisri HR, Nandini NM, Gujral S, Manjunath GV. Dermatopathic lymphadenitis in HIV. Indian J Sex Transm Dis AIDS. 2009;30:103–5.

55. Reynolds HM, Dunbar PR, Uren RF, Blackett SA, Thompson JF, Smith NP. Three-dimensional visualization of lymphatic drainage patterns in patients with cutaneous melanoma. Lancet Oncol. 2007;8:806–12.

56. Farkas L, Beiske K, Lund-Johansen F, Brandtzaeg P, Jahnsen FL. Plasmacytoid dendritic cells (natural interferon- alpha/beta-producing cells) accumulate in cutaneous lupus erythematosus lesions. Am J Pathol. 2001;159:237–43.

57. Bigley V, McGovern N, Milne P, Dickinson R, Pagan S, Cookson S, et al. Langerin-expressing dendritic cells in human tissues are related to CD1c+ dendritic cells and distinct from Langerhans cells and CD141high XCR1+ dendritic cells. J Leukoc Biol. 2015;97:627–34.